



OPEN

SUBJECT AREAS:
BREAST CANCER
CELL INVASIONReceived
8 July 2013Accepted
15 October 2013Published
14 November 2013Correspondence and
requests for materials
should be addressed to
L.Q.H. (huanglq@
tsinghua.edu.cn;
huanglq@sz.tsinghua.
edu.cn)* These authors
contributed equally to
this work.

The natural compound magnolol inhibits invasion and exhibits potential in human breast cancer therapy

Ying Liu^{1,2*}, Wei Cao^{1,2*}, Bo Zhang³, Yong-qiang Liu⁴, Zhong-yuan Wang^{1,2}, Yan-ping Wu^{1,2}, Xian-jun Yu⁴, Xu-dong Zhang^{1,2}, Ping-hong Ming^{1,2}, Guang-biao Zhou⁴ & Laiqiang Huang^{1,2}

¹School of Life Sciences, Tsinghua University, Beijing, 100084, China, ²The Shenzhen Key Laboratory of Gene & Antibody Therapy, State Key Laboratory of Health Science & Technology (prep), Center for Biotechnology & Biomedicine and Division of Life & Health Sciences, Graduate School at Shenzhen, Tsinghua University, Shenzhen, Guangdong, 518055, China, ³National Laboratory of Biomacromolecules, Institute of Biophysics, Chinese Academy of Sciences, Beijing, 100101, China, ⁴Division of Molecular Carcinogenesis and Targeted Therapy for Cancer, State Key Laboratory of Biomembrane and Membrane Biotechnology, Institute of Zoology, Chinese Academy of Sciences, Beijing, 100101, China.

Invasion and metastasis are the main causes of treatment failure and death in breast cancer. Thus, novel invasion-based therapies such as those involving natural agents are urgently required. In this study, we examined the effects of magnolol (Mag), a compound extracted from medicinal herbs, on breast cancer cells *in vitro* and *in vivo*. Highly invasive cancer cells were found to be highly sensitive to treatment. Mag markedly inhibited the activity of highly invasive MDA-MB-231 cells. Furthermore, Mag significantly downregulated matrix metalloproteinase-9 (MMP-9) expression, an enzyme critical to tumor invasion. Mag also inhibited nuclear factor- κ B (NF- κ B) transcriptional activity and the DNA binding of NF- κ B to MMP-9 promoter. These results indicate that Mag suppresses tumor invasion by inhibiting MMP-9 through the NF- κ B pathway. Moreover, Mag overcame the promoting effects of phorbol 12-myristate 13-acetate (PMA) on the invasion of MDA-MB-231 cells. Our findings reveal the therapeutic potential and mechanism of Mag against cancer.

Breast cancer is a major cancer commonly observed in women. Annually, over 1 million women worldwide are diagnosed with this disease, which is also the second most common cause of cancer-related deaths¹. Invasion and metastasis are the main reasons for the high mortality rates associated with breast cancer and are the leading causes of poor clinical outcomes^{2,3}. Invasion and metastasis consist of several interdependent processes, including uncontrolled growth of cancer cells, migration and invasion to distant sites of surrounding tissues, as well as adhesion, invasion, and colonization of other organs and tissues⁴. Compared with other types of breast cancers, patients with highly invasive breast cancers have poor disease-free survival because of the highly invasive behavior of their disease⁵. Therefore, control of invasion and metastasis is an important therapeutic target for breast cancers.

Previous studies have proven that increased expression of matrix metalloproteinases (MMPs) is involved in tumor invasion and metastasis in many cancer types^{6,7}. To date, over 20 human MMPs have been identified⁸. Among them, MMP-2 and MMP-9 are the enzymes most crucial to tumor invasion owing to their ability to degrade extracellular matrix (ECM) and basement membrane⁹. MMP-2 is always constitutively expressed in highly metastatic tumors. Meanwhile, MMP-9 can be induced by growth factors, cytokines, or xenobiotics such as phorbol 12-myristate 13-acetate (PMA) through transcription factors [nuclear factor- κ B (NF- κ B) and activator protein-1 (AP-1)]^{10,11}. MMP-9 is also sufficient or necessary for metastasis to brain tissue during breast cancer progression¹¹. Thus, MMP-9 can be a target of breast cancer therapy by suppressing breast cancer invasion.

Magnolia officinalis belongs to family Magnoliaceae and is distributed over China, Japan, and South Korea. *M. officinalis* is used as a folk remedy for gastrointestinal disorders, cough, acute pain, anxiety, and allergic diseases¹²⁻¹⁹. Magnolol (Mag; 5,5'-diallyl-2,2'-dihydroxybiphenyl), a hydroxylated biphenyl compound isolated from the root and stem bark of *M. officinalis*, is shown to have muscle relaxant, anti-oxidative, anti-atherosclerosis, anti-inflammatory, and anti-microbial effects. Mag also induces differentiation and calcium mobilization^{18,20,21}. Recent studies have shown that Mag exhibits anti-cancer properties by inhibiting proliferation, inducing differentiation and apoptosis, suppressing angiogenesis, countering metastasis, and reversing multidrug resistance²². Several signaling pathways have been implicated in the regulation of apoptosis by Mag²¹. However,



studies have shown that EGFR/PI3K/Akt²² and Wnt/beta-catenin signaling²³ are involved in Mag-induced apoptosis, but the mechanisms underlying the antitumor activity of Mag remain unknown. Whether Mag has potential clinical application and anti-breast cancer activity also require further investigation. In this study, we investigated the effect of Mag against human breast cancer and the mechanisms of Mag against highly invasive breast cancer.

Results

Effects of Mag on breast cancer cell lines. We first examined the cytotoxicity of Mag on human breast cancer cell lines and normal human mammary epithelial cells (MCF-10A). By the MTT assay, we found that Mag had moderate cytotoxicity to MCF-7, SK-BR3, MDA-MB-453, MDA-MB-435S, MDA-MB-231, and MDA-MB-468 cells

with an IC₅₀ of 24.79 μ M to 59.4 μ M. The IC₅₀ of MCF-10A was higher than those breast cancer cell lines. Among the tested breast cancer cell lines, highly invasive (MDA-MB-231 and MDA-MB-468) breast cancer cells were more sensitive to Mag than poorly invasive (MCF-7 and SK-BR3) cells (Figure 1B and Table 1). By the MTT and Trypan Blue exclusion assays, we found that Mag inhibited the cell proliferation and growth of highly invasive estrogen receptor negative (ER-) MDA-MB-231 (Figures 1C and 1E) and poorly invasive ER+ MCF-7 (Figures 1D and 1F) cells in a time- and dose-dependent manner. Mag also suppressed the clonogenic activity of these two cell lines (Figure 1G). These results suggested that Mag inhibited the anchorage-dependent (cell proliferation) and anchorage-independent (colony formation) growth of highly and poorly invasive breast cancer cells, with the

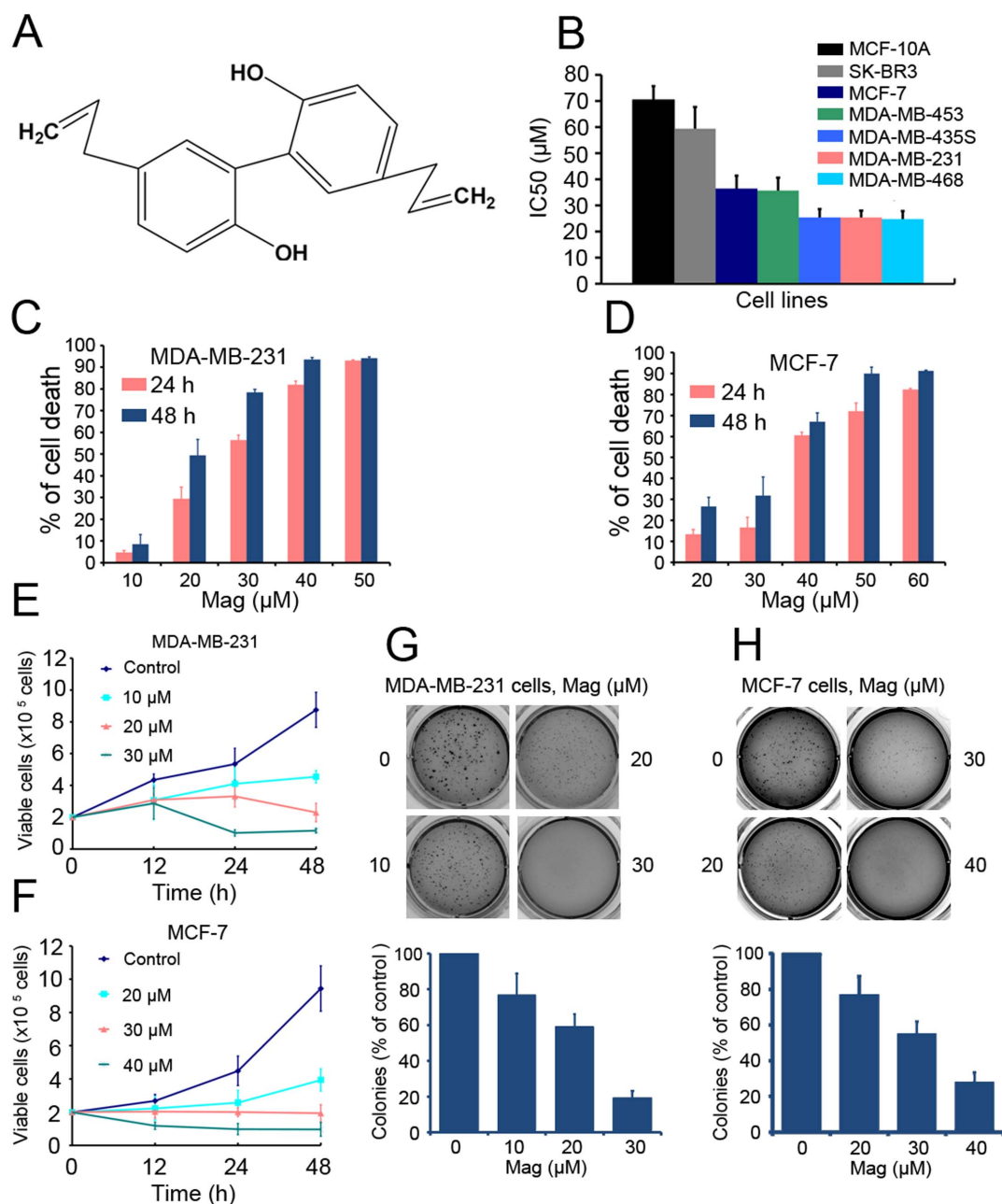


Figure 1 | Inhibitory effects of Mag on breast cancer cells. (A): Chemical structure of Mag. (B): The IC₅₀ of Mag for indicated cell lines. (C and D): The inhibitory effects of Mag on MDA-MB-231 and MCF-7 cells analyzed by MTT assay. (E and F): Inhibitory effects of Mag on cell viability of MDA-MB-231 and MCF-7 cells assayed by trypan blue exclusion assay. (G and H): The colony formation assays of MDA-MB-231 and MCF-7 cells treated with Mag at indicated concentration.

Table 1 | IC₅₀s of Mag on breast cancer cell lines

Cell lines	MCF-10A	SK-BR3	MCF-7	MDA-MB-453	MDA-MB-435S	MDA-MB-231	MDA-MB-468
IC ₅₀ (μM)	70.52 ± 5.09	59.40 ± 8.24	36.46 ± 2.38	35.69 ± 4.91	25.39 ± 3.26	25.32 ± 2.72	24.79 ± 3.06

[The cells were treated with Mag at various concentrations for 24 h, the cell cytotoxicity was analyzed by MTT assay, and the IC₅₀ was calculated using CalcuSyn (version 2.0, Biosoft, Cambridge, UK). Values shown are means plus or minus SD of quadruplicate determinations].

highly invasive breast cancer cells being more sensitive to treatment using Mag.

Effects of Mag on the invasion, migration, and adhesion of MDA-MB-231 cells. Considering that highly invasive breast cancer cells were more sensitive to treatment with Mag than poorly invasive cells, we next determined whether Mag inhibited the invasive behavior of breast cancer cells. The invasion assay was performed in highly invasive MDA-MB-231 cells using Matrigel-coated 24-well microchemotaxis chambers in the presence of Mag. As shown in Figure 2A, Mag (0 μM to 30 μM) markedly suppressed the invasion of MDA-MB-231 cells. To further explore the effect of Mag on migration,

MDA-MB-231 cells were treated with Mag (0 μM to 30 μM), and cell migration was determined after 24 h. As shown in Figure 2B, Mag significantly decreased MDA-MB-231 cell migration in a dose-dependent manner. Finally, we evaluated the effect of Mag on cell adhesion. As shown in Figure 2C, Mag also inhibited the adhesion of MDA-MB-231 cells onto the Matrigel in a concentration-dependent manner compared with the untreated control. These results suggested that Mag exhibited anti-invasive behavior toward breast cancer at non-cytotoxic concentrations.

Mag suppresses the invasion of MDA-MB-231 cells by inhibiting MMP-9 through the NF-κB pathway.

Cancer invasiveness and metastasis are associated with increased expression of MMPs^{11,24}. MMP-2 and MMP-9 are the key enzymes expressed in breast cancer cells, and their proteolytic activity contributes to cell invasion and metastasis^{25–27}. Therefore, we determined whether the inhibition of the invasive behavior of breast cancer cells by Mag can be mediated by suppressing MMP-2 and MMP-9 activities in MDA-MB-231 cells. Gelatin zymography was performed using the conditioned medium (CM) from the Mag-treated cells. As shown in Figure 3A, Mag markedly reduced the gelatinolytic activity of MMP-9 from MDA-MB-231 cells, suggesting that Mag inhibited the invasiveness of breast cancer cells by the inhibition of MMP-9 activity. Consistent with the inhibition of gelatinolytic activity, Western blot analysis of the CM also revealed that Mag downregulated the level of MMP-9 secretion (Figure 3B). To determine whether the inhibitory effect of Mag on MMP-9 secretion resulted from a downregulated level of *MMP-9* mRNA expression, real-time PCR was conducted. Results confirmed that Mag significantly downregulated *MMP-9* mRNA expression levels (Figure 3C). These results indicated that the Mag-mediated regulation of MMP-9 expression occurred at the transcriptional level, and the downregulation of MMP-9 inhibited the invasion of MDA-MB-231 cells.

The NF-κB and AP-1 pathways are critical transcription factors in the regulation of MMP-9 expression^{27,28}. To further understand the inhibitory mechanisms of Mag on *MMP-9* transcriptional regulation, the NF-κB and AP-1 pathways were investigated by Western blot analysis as well as reporter and ChIP assays. As shown in Figures 3D to 3F, Mag inhibited the phosphorylation of IκBα (pIκBα) and P65 (pP65) in MDA-MB-231 cells and prevented the translocation of P65 from cytoplasm to nucleus. This phenomenon indicated that IκBα degradation and P65 translocation from cytoplasm to nucleus was blocked by Mag. Mag inhibited NF-κB transcription activity at 20 and 30 μM (Figure 3G) and the DNA binding of NF-κB to *MMP-9* promoter at 20 μM (Figure 3H). AP-1, known to be regulated by MAPKs such as ERK, JNK, and P38 kinase, is another transcription factor involved in the activation of *MMP-9* transcription^{25,29}. Therefore, Mag may act through the AP-1 pathway to inhibit *MMP-9* gene expression. To investigate this possibility, we first examined the effect of Mag on the transcriptional activity of AP-1 and on the phosphorylation of MAPK family members. As shown in Figure 3I, Mag exerted no effect on AP-1 transcriptional activity. The phosphorylation of P38, ERK, and JNK was not significantly affected by Mag, and the respective total protein levels of these MAPKs remained unchanged (Figure 3J). These results indicated that the NF-κB pathway mediating *MMP-9* mRNA expression was

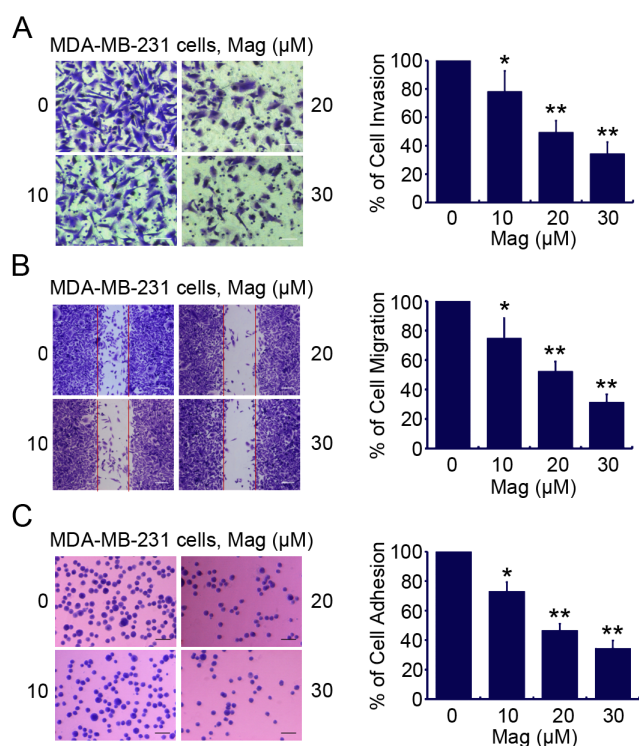


Figure 2 | Mag reduces the invasion, migration, and adhesion of MDA-MB-231 cells. (A): Invasion assay was carried out using modified 24-well microchemotaxis chambers. Then randomly chosen fields were photographed ($\times 100$), and the number of cells migrated to the lower surface was calculated as a percentage of invasion. Scale bar = 200 μm. Data are shown as the mean \pm SD of three independent experiments by analysis of Student's t test. *, $P < 0.05$, **, $P < 0.001$, vs 0 μM. (B): Confluent cells were scratched and then treated with Mag in a complete medium for 24 h. The number of cells migrated into the scratched area was photographed ($\times 40$) and calculated as a percentage of migration. Scale bar = 300 μm. Data are shown as the mean \pm SD of three independent experiments by analysis of Student's t test. *, $P < 0.05$, and **, $P < 0.001$, vs 0 μM. (C): Cells were seeded in a 96-well plate coated with matrigel and treated with Mag. Attached cells were photographed ($\times 100$) after crystal violet staining, and the number of attached cells was quantified by measuring O.D.. Scale bar = 80 μm. Data are shown as the mean \pm SD of three independent experiments. *, $P < 0.01$, **, $P < 0.001$ vs 0 μM.

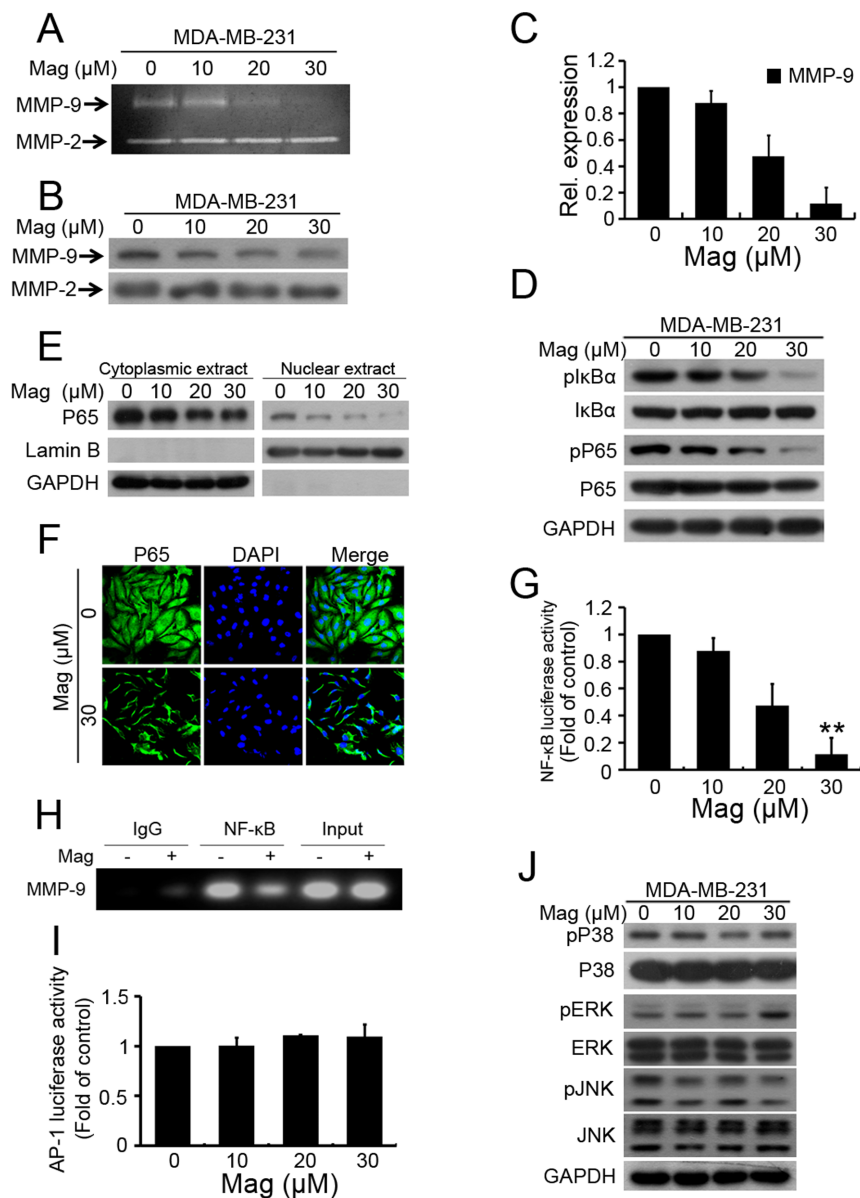


Figure 3 | Mag suppresses breast cancer cell invasion through the inhibition of *MMP-9* via NF- κ B pathway. MDA-MB-231 cells were treated with increasing concentrations of Mag for 24 h. (A): The activity of *MMP-9* was assessed using the concentrated conditioned medium (CM) by gelatin zymography. The concentration of CM protein was measured by Bradford assay. (B): Western blot was performed using antibodies indicated from CM of the Mag treated cells. The concentration of CM protein was measured by Bradford assay. (C): *MMP-9* gene expression was detected by Real-time PCR analysis. GAPDH was used here as a housekeeping gene. (D): MDA-MB-231 cells were treated with increasing concentrations of Mag for 24 h, Western blot was performed using antibodies indicated. (E): Cytoplasmic and nuclear fractions of MDA-MB-231 cells were isolated, the concentration of nuclear and cytoplasmic protein was measured by Bradford assay, the same amount of nuclear and cytoplasmic protein was subjected to SDS gel, and Western blot were performed with anti-P65, GAPDH and Lamin B antibodies. (F): MDA-MB-231 cells were treated with Mag at 0 and 30 μ M for 24 h. For immunofluorescence analysis, cells were stained with an anti-P65 antibody and DAPI and observed by confocal microscopy. (G): MDA-MB-231 cells were transfected with the NF- κ B luciferase reporter construct for 4 h and then treated with Mag. Luciferase activity was measured using the Luciferase assay system. (H): MDA-MB-231 cells treated with Mag (20 μ M) were processed for ChIP assay. Immunoprecipitation was performed with NF- κ B p65 or IgG as a control. The NF- κ B binding site of *MMP-9* promoter was detected by PCR. (I): MDA-MB-231 cells were transfected with the AP-1 luciferase reporter construct for 4 h and then treated with Mag. Luciferase activity was measured using the Luciferase assay system. (J): Western blot was performed using antibodies indicated. *, $P < 0.01$, **, $P < 0.001$ vs 0 μ M. (I): Real-time PCR analysis *MMP-9* expression lysates of tumor samples. **, $P < 0.001$ vs vehicle. (J): Western blot analysis of lysates of tumor samples using indicated antibodies. Full-length blots/gels are presented in Supplementary Figure 1 and 2.

inhibited by Mag, and Mag-induced invasive behavior inhibition was an NF- κ B-dependent event.

Mag overcame the promoting effects of PMA on the invasion of MDA-MB-231 cells. PMA has been shown to enable breast cancer cell invasion through the induction of the NF- κ B and/or AP-1 signaling pathways to mediate *MMP-9* transcription³⁰. Accordingly, we

determined whether Mag can abrogate the promoting effects of PMA on MDA-MB-231 cells. Interestingly, we found that Mag abrogated PMA-induced invasion (Figure 4A) by downregulating *MMP-9* gelatinolytic activity (Figure 4B), *MMP-9* mRNA expression (Figure 4C), and protein expression from CM (Figure 4D). We then examined the effects of Mag on NF- κ B and AP-1 signal cascades, which play a major role in *MMP-9* transcription. Our



results showed that in MDA-MB-231 cells, pI κ B α and pP65 were upregulated by treatment with PMA at 80 nM. Interestingly, pretreatment with Mag (0 μ M to 30 μ M for 12 h) markedly inhibited the PMA-induced upregulation of pI κ B α and pP65 (Figure 4E). In addition, we tested NF- κ B transcriptional activity by the luciferase reporter assay, and the result also showed that Mag significantly inhibited PMA-induced NF- κ B transcriptional activity (Figure 4F). We further investigated the effect of Mag on the PMA-induced upregulation of the phosphorylation of P38, ERK, and JNK as well as on AP-1 transcriptional activity

(Figures 4G and 4H). Results showed that Mag did not drastically affect the AP-1 signal cascades. These results indicated that Mag can overcome the facilitative effects of PMA on MDA-MB-231 cells by blocking NF- κ B-mediated *MMP-9* transcription. Taken together, our results demonstrated that the invasiveness of breast cells was weakened by a dose of Mag mainly through the NF- κ B signaling pathway, which regulates *MMP-9* (Figure 5).

Effect of Mag on breast cancer xenograft tumor growth *in vivo*. To evaluate the effect of Mag *in vivo*, MDA-MB-231 xenografted and

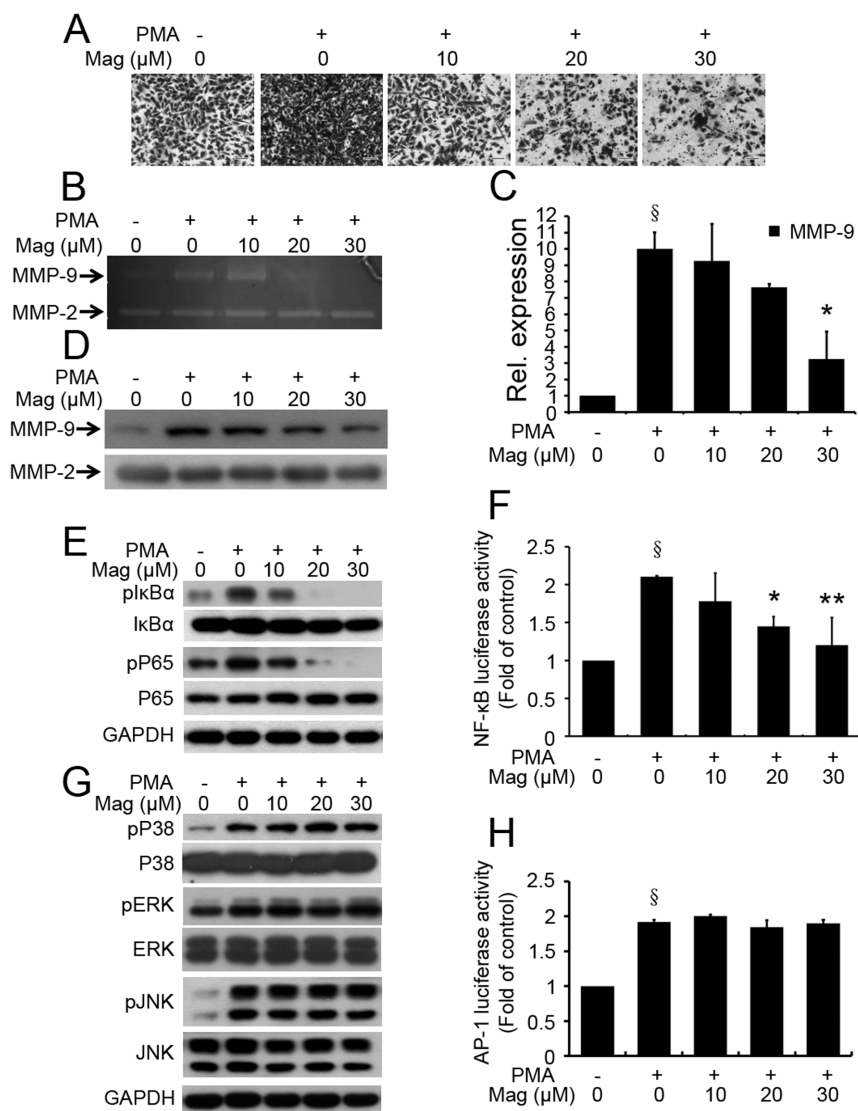


Figure 4 | Mag overcomes the facilitative effects of PMA on invasion of MDA-MB-231 cells. (A): MDA-MB-231 cells were preincubated with Mag for 30 min, and then cell suspension containing Mag and PMA (80 nM) was seeded onto the upper chamber wells. After incubation for 24 h at 37°C, the filter was fixed and stained with 0.2% crystal violet powder (15 min). Then randomly chosen fields were photographed ($\times 100$). Scale bar = 300 μ m. (B): MDA-MB-231 cells were pretreated with the indicated concentration of Mag for 30 min and then stimulated with 80 nM PMA for 24 h. The activity of MMP-9 was assessed using the concentrated CM by gelatin zymography. The concentration of CM protein was measured by Bradford assay. (C): MDA-MB-231 cells were pretreated with the indicated concentration of Mag for 30 min and then stimulated with 80 nM PMA for 24 h. *MMP-9* gene expression was detected by Real-time PCR analysis. GAPDH was used here as a housekeeping gene. (D): The protein expression of MMP-9 was assessed using the concentrated CM by Western blot. The concentration of CM protein was measured by Bradford assay. (E): Western blot was performed using antibodies indicated. (F): MDA-MB-231 cells transfected with pNF- κ B-luc reporter plasmid for 24 h were pretreated with Mag for 30 min and then exposed to PMA for another 20 h. NF- κ B firefly luciferase activity was measured using the Luciferase assay system. $\S P < 0.05$ vs control (without PMA treatment); * $P < 0.05$, ** $P < 0.01$ vs PMA-only group. (G): Western blot was performed using antibodies indicated. (H): MDA-MB-231 cells transfected with pAP-1-luc reporter plasmid for 24 h were pretreated with Mag for 30 min and then exposed to PMA for another 20 h. AP-1 firefly luciferase activity was measured using the Luciferase assay system. $\S P < 0.05$ vs control (without PMA treatment). Full-length blots/gels are presented in Supplementary Figure 3.

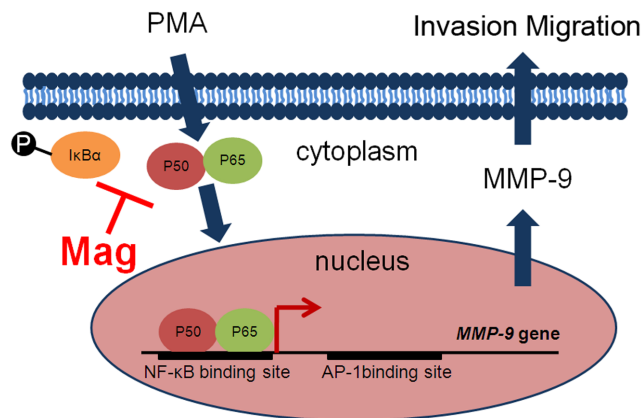


Figure 5 | Diagram of the signal pathway that Mag inhibits breast cancer cell invasion and migration.

MCF-7 xenografted murine models were generated. Tumor-bearing mice were treated with vehicle (MDA-MB-231 = 6; MCF-7 = 10) or Mag (MDA-MB-231 = 8; MCF-7 = 10) *i.p.* at 40 mg/kg four times a week for four weeks. Animals were humanely killed when their tumors reached 1.5 cm in diameter or when paralysis or a major compromise in their quality of life occurred. As shown in Figures 6A–D, Mag significantly inhibited MDA-MB-231 and MCF-7 tumor growth ($P < 0.05$). Moreover, treatment with Mag did not reduce the body weight of mice, suggesting that Mag had no toxicity effect (Figures 6E and 6F). The tumor samples of mice bearing MDA-MB-231 cells were isolated, cells were harvested, and experiments were conducted to determine whether Mag perturbed *MMP-9* expression *in vivo*. Interestingly, samples from mice treated with Mag showed downregulated *MMP-9* levels compared with tumor tissues from vehicle mice (Figures 6G and 6H). These results demonstrated that the administration of Mag had great potential in breast cancer therapy.

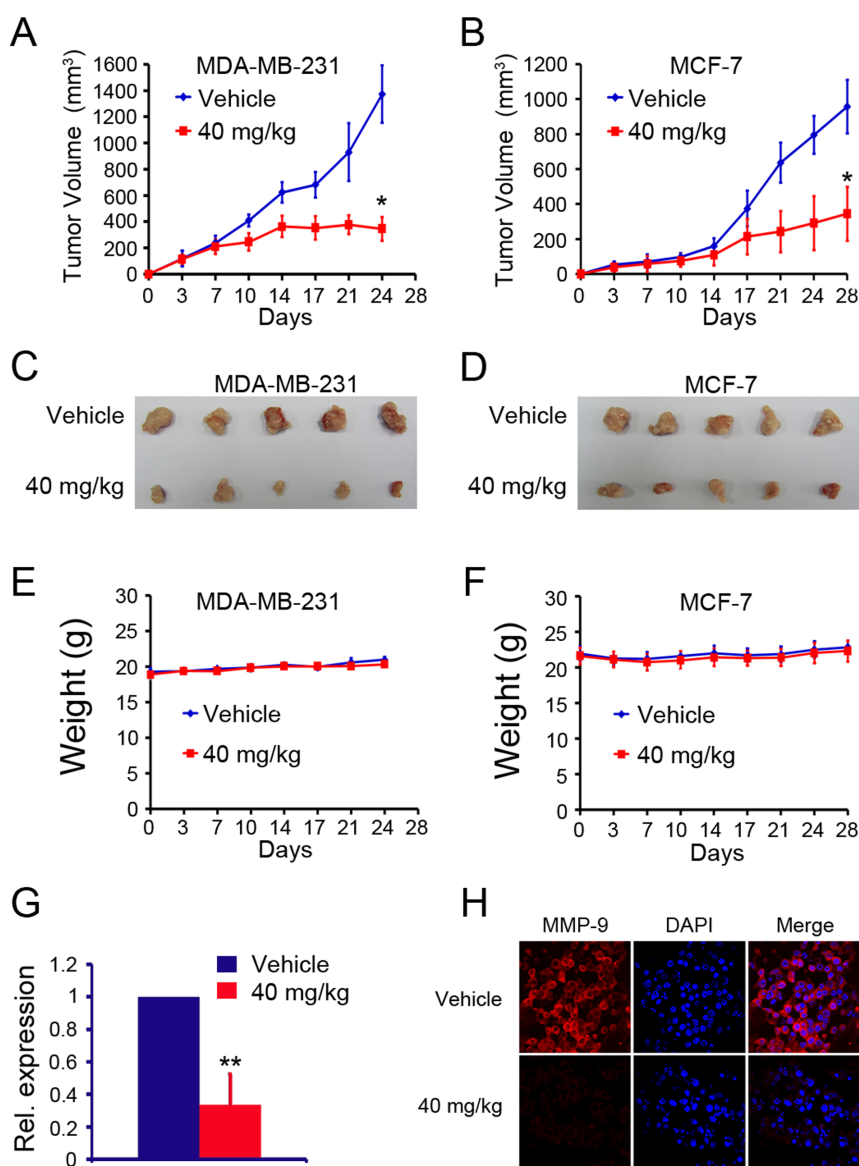


Figure 6 | *In vivo* therapeutic efficacy of Mag on human breast cancer murine models. (A)&(B): Mag significantly inhibited MDA-MB-231 and MCF-7 tumor growth. *, $P < 0.05$ vs vehicle. (C)&(D): Images of xenograft tumors obtained from mice. (E)&(F): Treatment with Mag did not affect animal body weight. (G)&(H): *MMP-9* expression in MDA-MB-231 tumor samples was detected by Real-time PCR and tumor immunofluorescence staining. **, $P < 0.001$ vs vehicle.



Discussion

Natural sources continue to provide front-line pharmacotherapy for millions of people worldwide^{18,21,22,31}. In this study, we reported for the first time the effect of Mag, a hydroxylated biphenyl compound isolated from the root and stem bark of *M. officinalis*, on the growth and invasive behavior of breast cancer cells. Several studies have documented the anti-cancer activity of Mag³¹. For example, Mag-induced apoptosis in HCT-116 colon cancer cells was associated with the AMP-activated protein kinase signaling pathway²⁰. In PC-3 prostate carcinoma cells, Mag reduced MMP-2/-9 and cyclooxygenase-2 at the mRNA level³². In the current work, we showed that Mag significantly inhibited breast cancer cell proliferation, growth, and colony formation, as well as suppressed tumor growth in a xenograft model of human breast cancer, suggesting its potential in breast cancer control.

Tumor invasion is a common feature of triple-negative breast cancers³³. Triple-negative breast cancers (12% to 24% of breast cancers)³⁴, which are characterized by the absence of ER, progesterone receptor, and HER-2 expression, result in high morbidity and mortality owing to their rapid growth rate, invasive potential, and frequently acquired treatment resistance. Migration and invasion are becoming important prerequisites of cancer progression and metastasis. Therefore, therapeutic strategies for preventing or suppressing cancer invasion and metastasis can significantly improve the survival of triple-negative breast cancer patients. The present data showed that Mag markedly inhibited the invasive (Figure 2A) and migratory (Figure 2B) abilities of MDA-MB-231 cells. In addition, the adhesion of cancer cells onto ECM and their interactions were crucial steps in the metastatic and invasion processes³⁵. We reported that Mag treatment markedly inhibited cell adhesion onto matrigel (Figure 2C).

MMPs are a family of metal-containing enzymes, and among them, MMP-2 and MMP-9 are highly expressed in invasive breast cancer cells^{11,25}. Evidence on the important role of MMP-9, known as a gelatinase B, in the invasive potential of tumors *in vitro* and *in vivo* has been reported^{25–27}. The current study demonstrated that Mag treatment inhibited the gelatinolytic activity and expression of MMP-9 at the protein and mRNA levels in MDA-MB-231 cells compared with untreated control (Figures 3A to 3C). Therefore, MMP-9 may be a Mag-responsive mediator whose degradation of ECM may cause subsequent cancer migration and invasion.

The *MMP-9* promoter region contains the cis-regulatory element, including one NF- κ B and two AP-1 binding sites^{36,37}. Thus, we investigated the effects of Mag on NF- κ B and AP-1 signal cascades, which play major roles in *MMP-9* transcription. The activation of NF- κ B confers growth/survival, invasion, and metastasis advantages, as well as drug resistance to many cancers³⁸. NF- κ B is activated by the phosphorylation-induced degradation of I κ B, which facilitates the dissociation of NF- κ B from I κ B family proteins. In this study, NF- κ B but not AP-1 was found to modulate Mag-reduced MMP-9 activity. Our results also demonstrated that Mag exerted anti-NF- κ B effect by blocking I κ B α phosphorylation and P65 phosphorylation without affecting total I κ B α and P65 expression (Figure 3D). Mag inhibited NF- κ B transcriptional activation (Figure 3G) and DNA binding to *MMP-9* promoter (Figure 3H). However, Mag exerted no effect on AP-1 transcriptional activation (Figure 3I). Parallel to this observation, the phosphorylation of ERK, JNK, and P38 kinase, which are known upstream molecules of AP-1, were unaffected by Mag (Figure 3J). Taken together, our findings demonstrated that the anti-invasive effect of Mag may be mediated by inhibiting NF- κ B-binding activities and suppressing the NF- κ B/I κ B pathway.

Previous studies have shown that PMA can be used as a tumor promoter in chemically induced carcinogenesis *in vitro* and *in vivo*^{25,29,39}. PMA can promote tumor migration and invasion by stimulating MMP-2 or MMP-9 expression through the induction of the NF- κ B and/or AP-1 signaling pathways in colon, hepatoma, glioma, and breast cancer cells¹⁰. To investigate the inhibitory effect

of Mag on PMA-induced MMP mRNA, we found that PMA induced the invasion of MDA-MB-231 (Figure 4A) breast cancer cells by inducing MMP-9 expression at both the mRNA and protein levels in a dose-dependent manner, indicating that impaired MMP-9 activity resulted from the downregulation of MMP-9 gene expression (Figures 4B to 4D). NF- κ B and AP-1 contributed to the effect of MMP-9 gene through PMA^{25,40}. As shown in Figures 4B to 4F, the inhibitory effect of Mag on MMP-9 enzyme activity at both mRNA and protein levels indicated that Mag abrogated the promoting effect of PMA on MDA-MB-231 cells by inhibiting NF- κ B signaling pathway-mediated *MMP-9* gene expression. However, Mag did not affect the stimulation of PMA on AP-1 and its upstream MAPK family members. Previous studies have reported that NF- κ B plays a regulatory role in PMA-induced *MMP-9* expression in breast cancer cells, whereas AP-1 exerted a negligible effect. Our data suggested that the NF- κ B pathway was the main regulatory pathway in suppressing PMA-induced MMP-9 gene expression and invasion by Mag.

In conclusion, the polyphenolic compound Mag isolated from traditional Chinese medicine inhibited the NF- κ B signaling pathway and resulted in the suppression of MMP-9 at the mRNA and protein levels. We also showed for the first time that Mag inhibited PMA-induced breast cancer cell invasion by MMP-9 expression. These findings suggested that this compound was a novel promising anti-cancer and anti-invasion compound. Moreover, Mag was a new potential therapeutic agent for patients with breast cancer, particularly highly invasive breast cancer.

Methods

Reagents. Mahanolol (Mag) with a purity of up to 98% was purchased from Shanghai Yuanye Bio-Technology Co., Ltd. Mag was dissolved in DMSO (Sigma) at a stock solution of 100 mM and stored at -20°C . Phorbol 12-myristate 13-acetate (PMA) was purchased from Sigma-Aldrich.

Cell culture. Human breast cancer cell lines MCF-7, MDA-MB-231, SK-BR3, MDA-MB-468, MDA-MB-453, and MDA-MB-435S and Non-tumorigenic MCF-10A human mammary epithelial cells were obtained from American Type Culture Collection (ATCC). MCF-7 and SK-BR3 cells were maintained in Dulbecco's modified Eagle's medium (DMEM)(Gibco) supplemented with 10% fetal bovine serum FBS (Hyclone) and antibiotics and incubated in a humidified atmosphere with 5% CO₂ at 37°C. MDA-MB-231 and MDA-MB-468 (triple-negative and highly invasive human breast cancer cell line), MDA-MB-453, and MDA-MB-435S cells were maintained in Leibovitz's-15 (L-15) (Gibco) supplemented with 10% FBS and antibiotics and incubated in a humidified atmosphere without CO₂ at 37°C. MCF-10A cells were maintained in DMEM/F12 medium containing 5% horse serum (HS), insulin (10 mg/ml), epidermal growth factor (EGF, 20 ng/ml), cholera toxin (100 mg/ml), hydrocortisone (0.5 mg/ml), penicillin (50 U/ml), and streptomycin (50 U/ml), and incubated in a humidified atmosphere without CO₂ at 37°C.

Cytotoxic assay and cell viability. Cells were seeded into 96-well plate and pre-cultured for 24 h, then treated with Mag for 24 or 48 h. Cell cytotoxicity was determined by MTT assay. The absorbance was measured at 570 nm by Automated Microplated Reader (Bio-Tek, VT, USA), and the cell death rate was calculated as followed: Cell death (%) = (average A₅₇₀ of the control group - average A₅₇₀ of the experimental group)/(average A₅₇₀ of the control group - average A₅₇₀ of the blank group) \times 100%²³. Cell viability was estimated by trypan blue dye exclusion⁴¹.

Soft-agar colony formation assay. Cells were suspended in 1 ml of DMEM or L-15 containing 0.3% low-melting-point agarose (Amresco, USA) and 10% FBS, and plated on a bottom layer containing 0.6% agarose and 10% FBS in 6-well plate in triplicate. After 2 weeks, plates were stained with 0.2% gentian violet and the colonies were counted under light microscope⁴².

Invasion assay. An invasion assay was carried out using 24-well plate (Corning). A polyvinyl-pyrrolidone-free polycarbonate filter (8 μm pore size) (Corning) was coated with matrigel (BD). The lower chamber was filled with medium containing 20% FBS as chemoattractant agents. The coated filter and upper chamber were laid over the lower chamber. Cells (1×10^4 cells/well) were preincubated with Mag for 30 min at room temperature, and then cell suspension containing Mag was seeded onto the upper chamber wells. After incubation for 20 h at 37°C, the filter was fixed and stained with 2% ethanol containing 0.2% crystal violet (15 min). After being dried, the stained cells were enumerated under light microscope at 10 \times objective. For quantification, the invaded stained cells on the other side of the membrane were extracted with 33% acetic acid. The absorbance of the eluted stain was determined at 570 nm.



Wound healing assay. Cells (4×10^5 cells/2 ml) were seeded in a 6-well plate and incubated at 37°C until 90% to 100% confluent. After the confluent cells were scratched with a 200 μ l pipet tip, followed by washing with PBS, and then treated with Mag in a complete medium. After 24 h of incubation, the cells were fixed and stained with 2% ethanol containing 0.2% crystal violet powder (15 min), and randomly chosen fields were photographed under a light microscope at 4 \times objective. The number of cells migrated into the scratched area was calculated.

Adhesion assay. Cells (5×10^4 cells/well) preincubated with Mag for 30 min at 37°C were seeded in a 96-well plate coated with matrigel for 20 min at 37°C. Unattached cells were removed by washing with PBS. Attached cells were fixed in 4% paraformaldehyde for 15 min, stained with 0.02% crystal violet solution for 10 min, and randomly chosen fields were photographed under a Leica DMI 400B microscope. Then, to quantify the number of attached cells, crystal violet was dissolved with 70% ethanol and O.D. was measured by microplate reader at 570 nm, reference 405 nm. The adhesion cells were calculated as a percentage of adhesion.

Gelatin zymography. MDA-MB-231 cells were seeded in 6-well plates and allowed to grow to 80% confluency. The cells were then maintained in serum-free medium for 12 h prior to designated treatments with Mag and PMA for 20 h. Conditioned medium was then collected, cleared and mixed with $5 \times$ SDS loading buffer, and subjected to electrophoresis on a 10% SDS-PAGE gel containing 0.1% gelatin. After electrophoresis, the gels were washed in renaturing buffer (pH 7.5, 2.5% Triton X-100) for 30 min, 4 times, and equilibrated in developing buffer (50 mM Tris-HCl pH 7.5, 10 mM CaCl₂, and 1 mM ZnCl₂) for 30 min and finally incubated in fresh developing buffer at 37°C for 24 h to allow digestion of the gelatin. The gelatinolytic activity of MMPs was visualized by staining the gels with 0.5% Coomassie blue R-250 in 45% methanol, 10% acetic acid and destained with 45% methanol, 10% acetic acid until clear bands suggestive of gelatin digestion appeared.

Real-time quantitative PCR. Expression of the *MMP-9* gene was examined by real-time polymerase chain reaction (PCR) normalized to expression of GAPDH. Total RNA was extracted from cell lines or patients' cells using Trizol reagent (Invitrogen). Quantitative real-time PCR was performed using SYBR Premix Ex Taq (Perfect Real Time) (TaKaRa Code: DRR041) according to the manufacturer's instruction⁴⁸. For real-time PCR, we used *MMP-9* gene forward primer 5'-GAGTGGCAGGGGAAGATGC-3', *MMP-9* gene reverse primer 5'-CCTCAGGCACTGCAGGATG-3'; *GAPDH* forward primer 5'-TGTTGCCATCAATGACCCCTT-3', *GAPDH* reverse primer 5'-CTCCACGACGTACTCAGCG-3'.

Western blot. Cell pellets were lysed in RIPA buffer containing 50 mM Tris pH 8.0, 150 mM NaCl, 0.1% SDS, 0.5% deoxycholate, 1% NP-40, 1 mM DTT, 1 mM NaF, 1 mM sodium vanadate, 1 mM PMSF (Sigma), and 1% protease inhibitors cocktail (Merk). Protein extracts were quantitated and loaded on 8% to 12% sodium dodecyl sulfate polyacrylamide gel, electrophoresed, and transferred to a PVDF membrane (Millipore). The membrane was incubated with primary antibody, washed, and incubated with horseradish peroxidase (HRP)-conjugated secondary antibody (Pierce). Detection was performed by using a chemiluminescent Western detection kit (Cell Signaling)⁴⁴. The antibodies used were anti-MMP-9, anti-Ik β , anti-P65 (Santa Cruz Biotechnology), anti-P38, anti-pP38 (Thr180/Tyr182), anti-ERK1/2, anti-pERK1/2 (Thr202/Tyr204), anti-JNK1/2, and anti-pJNK1/2 (Thr183/Tyr185) (Cell Signaling Technology), anti-pIk β (Ser32), anti-pP65 (Ser536), anti-MMP-2 (Epitomics), and anti-GAPDH (Sangon Biotech., AB10016) antibodies.

Isolation of nuclear and cytoplasmic fractionation. Nuclear and cytoplasmic extracts were prepared with the NE-PER Nuclear and Cytoplasmic Extraction Kit (Thermo Scientific). The purity of nuclear and cytoplasmic extracts was assessed by Western blot with anti-lamin B (cell signaling) and anti-GAPDH antibodies, respectively.

Immunofluorescence staining. MDA-MB-231 cells were incubated in the presence or absence of Mag for 24 h. Cells were then fixed and penetrated. A primary antibody against P65 was added at a dilution of 1:500 and incubated with cells at 4°C overnight. A FITC conjugated goat anti-rabbit IgG antibody was used as the secondary antibody. For visualization of cell nucleus, DAPI was used. Sections were observed using an Olympus laser scanning confocal microscope with an imaging software (Olympus Fluoview FV-1000, Tokyo, Japan).

NF- κ B and AP-1 luciferase reporter assay. MDA-MB-231 cells were seeded in 12-well culture plates. At a confluency of 70%, cells were transfected with the pNF- κ B-Luc or pAP-1-Luc plasmids (Beyotime Institute of Biotechnology) using the Lipofectamine 2000 (Invitrogen) according to manufacturer's instruction. After transfection for 4 h, the cells were treated with Mag for 20 h or pretreated with Mag for 30 min followed by PMA stimulation for another 20 h. Firefly luciferase activities were assayed using the Luciferase Assay System (Promega) according to the manufacturer's instructions.

Chromatin immunoprecipitation (ChIP) assay. MDA-MB-231 cells treated with Mag for 24 h were processed for ChIP assay using a ChIP-IT Express Enzymatic kit (Active Motif). Briefly, immunoprecipitation was performed with NF- κ B p65 or rabbit IgG as a control. The NF- κ B binding site of *MMP-9* promoter was detected by

PCR using the following primers: 5'-GACCAAGGGATGGGGGATC-3' and 5'-CTTGACAGGCAAGTGCTGAC-3'.

Human breast cancer xenograft experiments. Female nude immunodeficient mice (nu/nu), 6–8 weeks old, were purchased from Guangdong Province Medical Animal Center, and maintained and monitored in a specific pathogen-free environment. All animal studies were conducted according to protocols approved by the Tsinghua University Animal Care and Use Committee, complying with the rules of REGULATIONS FOR THE ADMINISTRATION OF AFFAIRS CONCERNING EX-PERIMENTAL ANIMALS (Approved by the State Council of China). The mice were injected subcutaneously with human breast cancer MDA-MB-231 cells (6×10^6) or MCF-7 (4×10^6) suspended in 100 μ l L-15 or DMEM media into the right flank of each mouse⁴⁵. Treatments were started when the tumors reached a palpable size. Mice were randomly divided into two groups ($n = 6-10$) and treated 4 times per week. The control group received vehicle (0.8% DMSO/12% Cremophor/8% Ethanol in normal saline), while another group received intraperitoneally (*i.p.*) injection of Mag (40 mg/kg). Caliper measurements of the longest perpendicular tumor diameters were performed twice a week to estimate the tumor volume, using the following formula: $4\pi/3 \times (\text{width}/2)^2 \times (\text{length}/2)$, representing the 3-dimensional volume of an ellipse. Animals were sacrificed when tumors reached 1.5 cm or if the mice appeared moribund to prevent unnecessary morbidity to the mice. At the time of the animals' death, tumors were excised, cells were lysed for Real-time PCR or immunofluorescence.

Tumor immunofluorescence staining. Surgically excised tumors were cryosectioned to 7 μ m thick sections. Then the frozen sections were thawed and fixed with 4% paraformaldehyde for 30 min. After blocking with 3% BSA/0.2% Triton X-100 in PBS for 1 h, sections were incubated with anti-MMP-9 antibody at 4°C overnight. Cy3 conjugated donkey anti-goat IgG antibody were used as the secondary antibody. For visualization of cell nucleus, DAPI was used. Sections were observed by Olympus confocal laser scanning microscope.

Statistical analysis. All experiments were repeated at least three times and the data were presented as the mean \pm SD unless noted otherwise. Differences between data groups were evaluated for significance using Student t-test of unpaired data or one-way analysis of variance and Bonferroni post-test. The tumor volume was analyzed with two-way ANOVA and independent sample t test using the software SPSS 12.0 for Windows (Chicago, IL). *P* values less than 0.05 indicate statistical significance.

- Lim, E. J. *et al.* Methylsulfonylmethane Suppresses Breast Cancer Growth by Down-Regulating STAT3 and STAT5b Pathways. *PLoS. One.* **7**, e33361 (2012).
- Weigelt, B., Peterse, J. L. & van, V. Breast cancer metastasis: markers and models. *Nat. Rev. Cancer* **5**, 591–602 (2005).
- Christofori, G. New signals from the invasive front. *Nature* **441**, 444–450 (2006).
- Jiang, J. *et al.* NAHA, a novel hydroxamic acid-derivative, inhibits growth and angiogenesis of breast cancer in vitro and in vivo. *PLoS. One.* **7**, e34283 (2012).
- Lee, H. J. *et al.* Oral administration of penta-O-galloyl-beta-D-glucose suppresses triple-negative breast cancer xenograft growth and metastasis in strong association with JAK1-STAT3 inhibition. *Carcinogenesis* **32**, 804–811 (2011).
- Rao, J. S. Molecular mechanisms of glioma invasiveness: the role of proteases. *Nat. Rev. Cancer* **3**, 489–501 (2003).
- Kim, Y., Kang, H., Jang, S. W. & Ko, J. Celastrol inhibits breast cancer cell invasion via suppression of NF- κ B-mediated matrix metalloproteinase-9 expression. *Cell Physiol Biochem.* **28**, 175–184 (2011).
- Clark, I. M., Swingler, T. E., Sampieri, C. L. & Edwards, D. R. The regulation of matrix metalloproteinases and their inhibitors. *Int. J. Biochem. Cell Biol.* **40**, 1362–1378 (2008).
- Park, S. Y., Kim, J. H., Lee, Y. J., Lee, S. J. & Kim, Y. Surfactin suppresses TPA-induced breast cancer cell invasion through the inhibition of MMP-9 expression. *Int. J. Oncol.* **42**, 287–296 (2013).
- Park, J. H. *et al.* Melittin suppresses PMA-induced tumor cell invasion by inhibiting NF- κ B and AP-1-dependent MMP-9 expression 1. *Mol. Cells* **29**, 209–215 (2010).
- Stark, A. M. *et al.* Differential expression of matrix metalloproteinases in brain- and bone-seeking clones of metastatic MDA-MB-231 breast cancer cells. *J. Neurooncol.* **81**, 39–48 (2007).
- Maruyama, Y., Kuribara, H., Morita, M., Yuzurihara, M. & Weintraub, S. T. Identification of magnolol and honokiol as anxiolytic agents in extracts of saiboku-to, an oriental herbal medicine. *J. Nat. Prod.* **61**, 135–138 (1998).
- Wang, J. P. *et al.* Anti-inflammatory and analgesic effects of magnolol. *Naunyn Schmiedebergs Arch. Pharmacol.* **346**, 707–712 (1992).
- Seo, J. U., Kim, M. H., Kim, H. M. & Jeong, H. J. Anticancer potential of magnolol for lung cancer treatment. *Arch. Pharm. Res.* **34**, 625–633 (2011).
- Tse, A. K. *et al.* Magnolol suppresses NF- κ B activation and NF- κ B regulated gene expression through inhibition of IkappaB kinase activation. *Mol. Immunol.* **44**, 2647–2658 (2007).
- Bang, K. H. *et al.* Antifungal activity of magnolol and honokiol. *Arch. Pharm. Res.* **23**, 46–49 (2000).
- Ho, K. Y., Tsai, C. C., Chen, C. P., Huang, J. S. & Lin, C. C. Antimicrobial activity of honokiol and magnolol isolated from *Magnolia officinalis*. *Phytother. Res.* **15**, 139–141 (2001).



18. Fong, W. F., Tse, A. K., Poon, K. H. & Wang, C. Magnolol and honokiol enhance HL-60 human leukemia cell differentiation induced by 1,25-dihydroxyvitamin D3 and retinoic acid. *Int. J. Biochem. Cell Biol.* **37**, 427–441 (2005).
19. Zhai, H., Nakade, K., Mitsumoto, Y. & Fukuyama, Y. Honokiol and magnolol induce Ca²⁺ mobilization in rat cortical neurons and human neuroblastoma SH-SY5Y cells. *Eur. J. Pharmacol.* **474**, 199–204 (2003).
20. Hwang, E. S. & Park, K. K. Magnolol suppresses metastasis via inhibition of invasion, migration, and matrix metalloproteinase-2/-9 activities in PC-3 human prostate carcinoma cells. *Biosci. Biotechnol. Biochem.* **74**, 961–967 (2010).
21. Lee, D. H., Szczepanski, M. J. & Lee, Y. J. Magnolol induces apoptosis via inhibiting the EGFR/PI3K/Akt signaling pathway in human prostate cancer cells. *J. Cell Biochem.* **106**, 1113–1122 (2009).
22. Kang, Y. J. *et al.* Wnt/beta-catenin Signaling Mediates the Antitumor Activity of Magnolol in Colorectal Cancer Cells. *Mol. Pharmacol.* (2012).
23. Yu, X. J. *et al.* Gambogic acid induces G1 arrest via GSK3beta-dependent cyclin D1 degradation and triggers autophagy in lung cancer cells. *Cancer Lett.* **322**, 185–194 (2012).
24. Kessenbrock, K., Plaks, V. & Werb, Z. Matrix metalloproteinases: regulators of the tumor microenvironment. *Cell* **141**, 52–67 (2010).
25. Kim, Y., Kang, H., Jang, S. W. & Ko, J. Celastrol inhibits breast cancer cell invasion via suppression of NF-kB-mediated matrix metalloproteinase-9 expression. *Cell Physiol Biochem.* **28**, 175–184 (2011).
26. Ling, H., Yang, H., Tan, S. H., Chui, W. K. & Chew, E. H. 6-Shogaol, an active constituent of ginger, inhibits breast cancer cell invasion by reducing matrix metalloproteinase-9 expression via blockade of nuclear factor-kappaB activation. *Br. J. Pharmacol.* **161**, 1763–1777 (2010).
27. Lin, C. W. *et al.* Quercetin inhibition of tumor invasion via suppressing PKC delta/ERK/AP-1-dependent matrix metalloproteinase-9 activation in breast carcinoma cells. *Carcinogenesis* **29**, 1807–1815 (2008).
28. Woo, J. H. *et al.* Resveratrol inhibits phorbol myristate acetate-induced matrix metalloproteinase-9 expression by inhibiting JNK and PKC delta signal transduction. *Oncogene* **23**, 1845–1853 (2004).
29. Liu, J. F., Crepin, M., Liu, J. M., Barritault, D. & Ledoux, D. FGF-2 and TPA induce matrix metalloproteinase-9 secretion in MCF-7 cells through PKC activation of the Ras/ERK pathway. *Biochem. Biophys. Res. Commun.* **293**, 1174–1182 (2002).
30. Corson, T. W. & Crews, C. M. Molecular understanding and modern application of traditional medicines: triumphs and trials. *Cell* **130**, 769–774 (2007).
31. Park, J. B. *et al.* Magnolol-induced apoptosis in HCT-116 colon cancer cells is associated with the AMP-activated protein kinase signaling pathway. *Biol. Pharm. Bull.* **35**, 1614–1620 (2012).
32. Karroum, A. *et al.* Matrix metalloproteinase-9 is required for tubular network formation and migration of resistant breast cancer cells MCF-7 through PKC and ERK1/2 signalling pathways. *Cancer Lett.* **295**, 242–251 (2010).
33. Stevens, K. N., Vachon, C. M. & Couch, F. J. Genetic susceptibility to triple-negative breast cancer. *Cancer Res.* **73**, 2025–2030 (2013).
34. Lee, W. J., Chen, W. K., Wang, C. J., Lin, W. L. & Tseng, T. H. Apigenin inhibits HGF-promoted invasive growth and metastasis involving blocking PI3K/Akt pathway and beta 4 integrin function in MDA-MB-231 breast cancer cells. *Toxicol. Appl. Pharmacol.* **226**, 178–191 (2008).
35. Delassus, G. S., Cho, H., Park, J. & Eliceiri, G. L. New pathway links from cancer-progression determinants to gene expression of matrix metalloproteinases in breast cancer cells. *J. Cell Physiol* **217**, 739–744 (2008).
36. Aggarwal, B. B. Nuclear factor-kappaB: the enemy within. *Cancer Cell* **6**, 203–208 (2004).
37. Lee, C. H., Jeon, Y. T., Kim, S. H. & Song, Y. S. NF-kappaB as a potential molecular target for cancer therapy. *Biofactors* **29**, 19–35 (2007).
38. Kang, H. *et al.* N-(4-hydroxyphenyl)retinamide inhibits breast cancer cell invasion through suppressing NF-KB activation and inhibiting matrix metalloproteinase-9 expression 1. *J. Cell Biochem.* **113**, 2845–2855 (2012).
39. Lin, C. W., Shen, S. C., Hou, W. C., Yang, L. Y. & Chen, Y. C. Heme oxygenase-1 inhibits breast cancer invasion via suppressing the expression of matrix metalloproteinase-9. *Mol. Cancer Ther.* **7**, 1195–1206 (2008).
40. Park, S. K. *et al.* Kalopanaxsaponin A inhibits PMA-induced invasion by reducing matrix metalloproteinase-9 via PI3K/Akt- and PKCdelta-mediated signaling in MCF-7 human breast cancer cells 1. *Carcinogenesis* **30**, 1225–1233 (2009).
41. Zhang, B. *et al.* Gefitinib Analogue V1801 Induces Apoptosis of T790M EGFR-Harboring Lung Cancer Cells by Up-Regulation of the BH-3 Only Protein Noxa. *PLoS. One.* **7**, e48748 (2012).
42. Ma, L. *et al.* Overexpression and small molecule-triggered downregulation of CIP2A in lung cancer. *PLoS. One.* **6**, e20159 (2011).
43. Liu, Y. Q. *et al.* Identification of an Annonaceous Acetogenin Mimetic, AA005, as an AMPK Activator and Autophagy Inducer in Colon Cancer Cells. *PLoS. One.* **7**, e47049 (2012).
44. Bin Liu *et al.* ABL-N-induced apoptosis in human breast cancer cells is partially mediated by c-Jun NH2-terminal kinase activation. *Breast Cancer Research* **12**, R9 (2010).
45. Rao, J. S. Molecular mechanisms of glioma invasiveness: the role of proteases. *Nat. Rev. Cancer* **3**, 489–501 (2003).

Acknowledgements

This work was supported by funding to L.H. from China MOST National Key Basic Research 973 Program (2005CCA03500), China NSFC (30570960), Guangdong Province NSF (05010197), and Shenzhen Municipal Science & Technology Programs for Building State and Shenzhen Key Laboratories (2006464, 200712, SG200810150043A, CXB201005260070A, CXB201104220043A, ZDSY20120616222747467).

Author contributions

L.H. conceived the research; Y.L. and L.H. designed the project; Y.L., W.C. and B.Z. performed most of the experiments; Y.L., Z.W. and Y.W. performed some of the experiments; P.M. helped to construct murine model; X.Y., X.Z. and G.Z. provided some of the reagents and advice; Y.L. and L.H. wrote the manuscript; all authors reviewed the manuscript.

Additional information

Supplementary information accompanies this paper at <http://www.nature.com/scientificreports>

Competing financial interests: The authors declare no competing financial interests.

How to cite this article: Liu, Y. *et al.* The natural compound magnolol inhibits invasion and exhibits potential in human breast cancer therapy. *Sci. Rep.* **3**, 3098; DOI:10.1038/srep03098 (2013).



This work is licensed under a Creative Commons Attribution-NonCommercial-NoDerivs 3.0 Unported license. To view a copy of this license, visit <http://creativecommons.org/licenses/by-nc-nd/3.0>